Hindawi
Advances in Materials Science and Engineering
Volume 2022, Article ID 7852652, 12 pages
https://doi.org/10.1155/2022/7852652

Research Article

Multilevel Structural Characteristics of Jinshajiang Main Fault and Its Influence on Engineering

Hui Zhou[1,2], **Yihuan Shen**[1,2], **Yong Zhu**[1,2], **Gang Han**[1,2], **Chuanqing Zhang**[1,2] and **Ning Zhang**[1,2]

[1]*State Key Laboratory of Geomechanics and Geotechnical Engineering, Institute of Rock and Soil Mechanics, Chinese Academy of Sciences, Wuhan 430071, China*
[2]*University of Chinese Academy of Sciences, Beijing 100049, China*

Correspondence should be addressed to Hui Zhou; hzhou@whrsm.ac.cn

Received 18 December 2021; Accepted 15 January 2022; Published 8 March 2022

Academic Editor: Yonghong Wang

It is of great significance to study the geological characteristics of faults and the corresponding displacement patterns for the tunnel engineering crossing active faults. On the basis of field investigation and geological data analysis, it is found that the secondary weak structures, such as narrow cleavage bands, narrow joint bands, fault gouge zones, and small folds, often appear in the fault fracture zones and affected zones. The multilevel structure of fault is proposed from mechanics and engineering by summarizing their main characteristics. Taking the outcrop of fracture zones of Batang section, Jinshajiang main fault in the Qinghai-Tibet Plateau as the research object, the geometric characteristics of rock masses, the particle size, mineral composition, and mechanical characteristics of rocks in the fault are studied through field investigation, geological mapping, mineral composition analysis, and mechanical tests. In addition, a displacement model of multilevel structure fault is presented by numerical simulation. The results show that the Jinshajiang main fault comprises a primary structure and several secondary weak structures, which has a typical structure of multilevel fault. There are several secondary weak structures in the outcrop of the fracture zone. Compared with the rock masses in the primary structure, the joints of the rock masses in the secondary weak structure are more developed, and the rock particle size is smaller, the mud content is higher, and the mechanical strength is lower. The geometric morphology, mineral composition, and mechanical properties of the rock masses in the secondary weak structure are obviously different from those of the primary structure. The overall displacement mode of multilevel structural fault is S-shaped distribution, and the secondary weak structure will affect the displacement distribution pattern and have the possibility of sliding when the fault moves. Therefore, the secondary weak structure section in the tunnel should be a priority for prevention and control when designing tunnels through active faults. The multilevel structure of the fault, together with centralized structure, distributed structure, and stepped structure of the fault, can be used as a structure classification method of fault structure, which provides a reference for the study of disaster mechanisms, and prevention and control measures of tunnels crossing active faults.

1. Introduction

With the rapid increase in the scale of tunnel construction globally, it is inevitable that tunnel engineering will pass through active faults and face the risk of structural damage caused by the slip of the fault. Understanding faults from engineering scale is one of the bases for studying disaster prevention and control of tunnels crossing active faults. The fault structure and its physical and mechanical properties determine the distribution of fault displacement along the axial direction of the tunnel, and the displacement gradient of the surrounding rocks relative to the tunnel is one of the decisive factors for the failure of the tunnel. Therefore, it is essential to comprehend the structural characteristics of faults and the corresponding displacement patterns for the construction and operation safety of tunnels crossing active faults.

In view of the structural characteristics and displacement patterns of faults, there are three main structural types of faults on the engineering scale: centralized structure, distributed structure, and stepped structure [1]. Centralized

structural faults, also known as blade structural faults, such as the Lisan Peninsula fault [2], are characterized by frictional sliding of two walls of rock masses along the section. Distributed structural faults, also known as deformation zone faults, such as the Dadong fault in Utah [3], manifest as an S-shaped distribution of fault displacement along the deformation zone. Stepped structural faults, also called faults with multiple fracture surfaces, such as the Gullfaks oil field in the northern North Sea [4], are manifested by the sliding of the rock mass along multiple nearly parallel fault planes. With the advance of geological investigation, in the field outcrops of many large faults, the secondary weak structures including joint fracture zones, cleavage zones, and clay zones have been discovered in the fracture zone outside the fault core or in the affected zone. For example, secondary fault gouges interspersed in the fracture zone were found in the Hayward fault of the Berkeley Mountain Tunnel in the United States [5]; at the outcrop of the fault in the Huangcaoping Tunnel site, small faults of 0.4~2 m width, compressocrushed zone, and other secondary weak structures can be seen every few meters or tens of meters [6]; the Carboneras fault in southeastern Spain has detected multiple secondary fault gouges several meters wide [7], and the Caleta Coloso fault in northern Chile has discovered multiple secondary ultracataclasite zones [7]. Many active faults with a certain scale (mostly 100-meter width) have developed one or several secondary weak structures in their fracture zone or affected zone. However, this kind of fault structure has not attracted enough attention from the industrial and academic fields. At present, many scholars' research on tunnel engineering crossing active faults is mainly based on centralized structural faults and distributed structural faults [8–11]. However, there are few studies on the physical and mechanical properties of faults with weak structures and their impact on engineering, which is of great engineering instructive significance to slip-resistant design of tunnels crossing active faults.

On the basis of numerous fault geological survey data and the field investigations results of the Jinshajiang main fault, the fault multilevel structure is proposed from the perspective of engineering and mechanics. Taking the Batang section of the Jinshajiang main fault as a typical case, the difference between rock masses of the secondary weak structure dominated by fault gouges and that of main structure has been comprehensively explored in terms of geometric structure, mineral composition, and mechanical properties through geological surveys, laboratory test, and numerical simulations. The main characteristics and displacement patterns of the multilevel structure of fault are summarized, and the corresponding engineering prevention and control suggestions are proposed. The research results can provide references for the study of disaster mechanisms and prevention and control measures for tunnels crossing active faults.

2. The Concept and Research Method of Fault Multilevel Structure

2.1. Fault Multilevel Structure. The Jinshajiang main fault, the Carboneras fault [7], and many other faults of a certain scale have developed one more fault gouge, ultracataclastic rocks, small folds, and other secondary weak structures in the fracture zone or affected zone outside the fault core. A fault core is usually an area in the center of the fault where only the remnants of the original rock structure are preserved [12], ranging in thickness from millimeters to meters. Some scholars in geology consider the secondary weak structure as the fault core and call the fault structure which contains many fault cores in the fracture zone the "multiple cores model" [13], thus analyzing the influence of the structure on the mechanical properties and fluid migration of the crust. However, in engineering, the focus is the physical and mechanical properties of different parts of the fault and fault displacement patterns. It is necessary to preliminarily judge the key points of fortification from the geometric characteristics and thus provide a basis for the design of tunnels crossing active faults in terms of mechanical classification, displacement concentration, and activity characteristics. Therefore, the fault multilevel structure is proposed from the perspective of engineering and mechanics, and this structure is regarded as a form of fault structure juxtaposed with centralized structure, distributed structure, and stepped structure.

The fault multilevel structure means that the fault contains the primary structure and the secondary weak structure. From the fault core, the primary structure is followed by the fracture zone, the affected zone, and the hanging wall or foot wall (Figure 1). The secondary weak structure refers to the area with weak mechanical properties such as narrow cleavage band, joint narrow band, fault gouge, and small fold outside the fault core, which are more common in the fracture zone and affected zones with the width varying from several meters to more than ten meters.

Faults of a certain scale are often formed by multiple periods of geological activity. The secondary weak structure in the fracture zone or the affected zone may be formed by old stage and current or multistage geological activities and may be formed before, during, and after the formation of the primary structure [12]. It is possible to form a sliding surface when the fault is active. There will be certain differences in the intensity of tectonic movement and the fracture center of the rock mass in different periods, which will result in the differences of the rupture and deformation degree of the fault in different positions. This is the dynamic basis for the formation of the multilevel structure. In each period of geological activities, the original rock at different locations is subject to different degrees of repeated crushing and fracture as well as the physical and chemical effects of water, resulting in differences in the mineral composition, fracture density, mechanical properties, and stress states of rocks at different locations. This is the material basis for the formation of the multilevel structure. For the primary structure, the integrity degree of the rock gradually increases from the fault core, and the strength of the rock under the same type of bedrock gradually increases, and the ability of resisting deformation is also stronger. The secondary weak structure is attached to the primary structure, but its geometric form and mechanical characteristics are clearly distinguished from those of the surrounding primary structure. The secondary weak

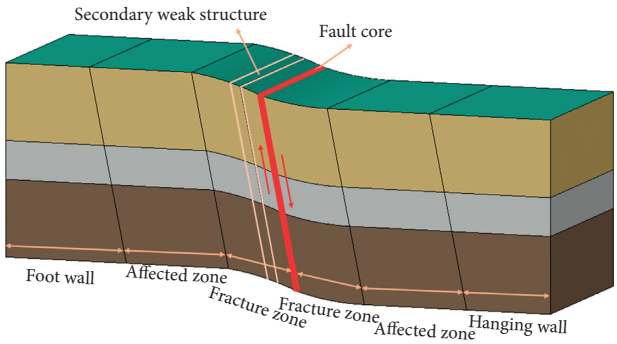

Figure 1: Geological zoning model of fault multilevel structure.

structure under fault dislocation will affect the deformation characteristics of the tunnel surrounding rock and the distribution of the surrounding stress field.

2.2. Research Methods. The Jinshajiang main fault is about 1200 km in length and about 50~70 km in width [14, 15]. The area is so large that it is difficult to investigate all of them. In this study, the outcrop of the fracture zone in the Batang section is selected for investigation. The primary structure and the secondary weak structure of the outcrop are considered as the representative characteristics of the multilevel structure of the fault. The safety problems of tunnel crossing the active fault are also analyzed according to these characteristics.

Physical test and numerical analysis are widely used in geotechnical engineering [16–21]. In this paper, the topography and mountain trend of the Batang section of the Jinshajiang main fault are studied, with emphasis on the outcrops of natural rocks in the area. Then take pictures of the outcrop every 2 m. Concatenate the photographs into a more than 50-meter-long photograph, and perform geological structure identification and geological sketches on key parts in order to understand the geometric characteristics of the multilevel structure. Typical rock samples of the secondary weak structure and the fracture zone were taken by geological hammer, and their particle sizes were compared. The powder of rock samples was then tested by X-ray diffraction to analyze its mineral composition so as to recognize the physical characteristics of fault multilevel structure. Later, the rock samples were subjected to point load test, and the large rock samples were processed into standard cubes for shear test to obtain the uniaxial compressive strength and shear strength of the rocks in the fracture zone of the Batang section of the Jinshajiang main fault. For the secondary weak structure represented by fault gouge, the mechanical strength range is obtained through the relevant literature so as to understand the mechanical characteristics of the fault multilevel structure. Finally, the finite difference method is used to analyze the influence of the secondary weak structure on the whole displacement mode during the creep sliding of typical fault multilevel structure.

Due to the limited site survey conditions and considering the feasibility of field research, this study cannot fully reveal the structural characteristics of the entire section of the Batang section of the Jinshajiang main fault whereas it aims to fully understand the characteristics of the multilevel structure through the detailed study of partial sections, thus providing a basis for subsequent research and a reference for tunnel engineering design.

3. Structural Features of Jinshajiang Fault Outcrop

3.1. Regional Tectonic Background. The Jinshajiang fault zone is a suture structure located at the northwest boundary of the Sichuan-Yunnan rhombic block [22, 23]. It is composed of three main faults and some secondary faults (Figure 2), and its total length is about 1200 km. It strikes north-south trend slightly protruding to the east and the arc top is near Batang [14, 15]. After a long period of tectonic evolution, it has the characteristics of multiperiod activity and complex geological structure.

Due to the geological movement, active faults have been divided into segmented ones. The Jinshajiang fault zone can be roughly divided into three sections: the north section, the middle section, and the south section, with the Batang fault and the Deqin-Zhongdian-Daju fault being their boundaries [14]. The study area is located in Litang County, Ganzi Tibetan Autonomous Region, Sichuan Province, in the middle section of the Jinshajiang fault zone. This fault is the Jinshajiang main fault, also known as the Lifu-Riyu fault, about 700 km long. Xu et al. [24] used the GPS velocity field in the Jinshajiang fault zone from 1991 to 2015 to give a dextral strike-slip rate of about 4.9 mm/a in the middle section of the Jinshajiang fault zone, and the dip-slip motion is weak. The profile of the fracture is a V-shaped canyon landform with low elevation nearby and high mountains on both sides. As shown in Figure 2, the mountains on both sides are obviously dislocated. The coordinates of the observed outcrop are 99.3278 longitude, 29.3803 latitude, and an altitude of about 3,230 m, which is within the range of the fracture zone in the western part of the Jinshajiang main fault.

3.2. Geometric Features. The observed outcrop is located on the side of the mountain road. The exposed rock is 2.5~3.5 m high and extends about 100 meters long. The outcrop is mainly brownish-yellow, and some rocks are light gray and dark gray. Overall, the outcrop rocks have relatively well-developed joints and belong to the fracture zone of the Jinshajiang main fault. Figure 3 shows a stitched photo of a 45 m outcrop. The investigation of the outcrops found that there are three secondary weak structures, namely, secondary weak structure A, secondary weak structure B, and secondary weak structure C in Figure 3, whose strike is almost the same as that of Jinshajiang fault zone, to the north-south direction.

The secondary weak structure A (Figure 4) is a small fault with a width of about 2.6 m and its boundary judged by the color and the size of the rock mass. The rock mass is in a plume pattern, with well-developed joints, and the distance between structural planes is less than 0.2 m, most of which are cemented together by the fractured structure and scattered structure. There have been two phases of movement:

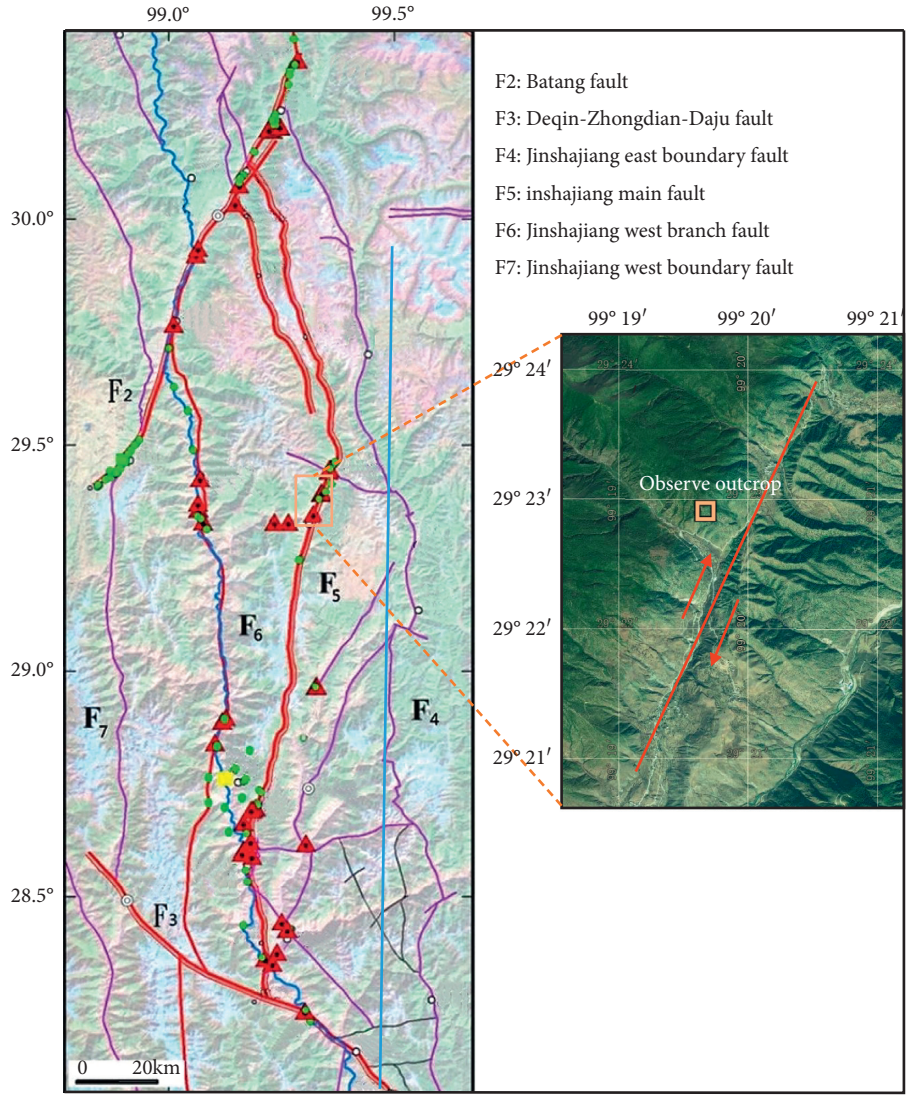

Figure 2: Jinshajiang fault zone [14] and observed outcrop location.

the nearly vertical strike-slip movement and the dip-slip movement with an inclination angle of about 24°. There are two typical products of fault activity in the secondary weak structure (Figure 5), one is fault gouge, which is light gray with curved strips, and the other is lens body, which is brown and lenticular.

The secondary weak structure B (Figure 6) is composed of a series of alternately developed limestone belts with dense joints and fault gouge belts, about 3 m wide. The secondary weak structure C (Figure 7) is about 2.5 m wide and is mainly composed of fault gouges. Both structures are created due to the vertical strike-slip movement. The bedding of the two faults shows obvious bending deformation, and its shape is similar to folds, which may be influenced by the dragging force due to the sliding of the rock mass.

3.3. Analysis of Particle Size and Mineral Composition. From the deep bottom to the surface outcrop, the formation rate of fault gouge and surrounding breccia has a decreasing trend [25], but outcrop characteristics, rock grain size, and the thickness of fault gouge can still reflect a great deal of information about the main fault dislocation. The samples were collected from 6 mark points in the secondary weak structure A (points 1~6 in Figure 4), 2 mark points in the fracture zone (points 7~8 in Figure 3), and 3 mark points in the secondary weak structure C (Points 9~11 in Figure 7). Figure 8 shows the rock samples of the secondary weak structure A and the secondary weak structure C, and Figure 9 shows the rock sample of the fracture zone. The rock samples are then placed on white paper with a length of 29.7 cm and a width of 21 cm. The samples shown in the figures are the most representative rock samples at the sampling point, which can reflect the characteristics of rock particle size at different locations. In the secondary weak structure A, the particle size at point 2 (fault gouge) is mostly in the range of 5–20 mm, and the breccia particle size tends to increase from point 2 to the outside. Based on the results of field observations, it is found that the degree of fragmentation of the secondary weak structure of the Jinshajiang

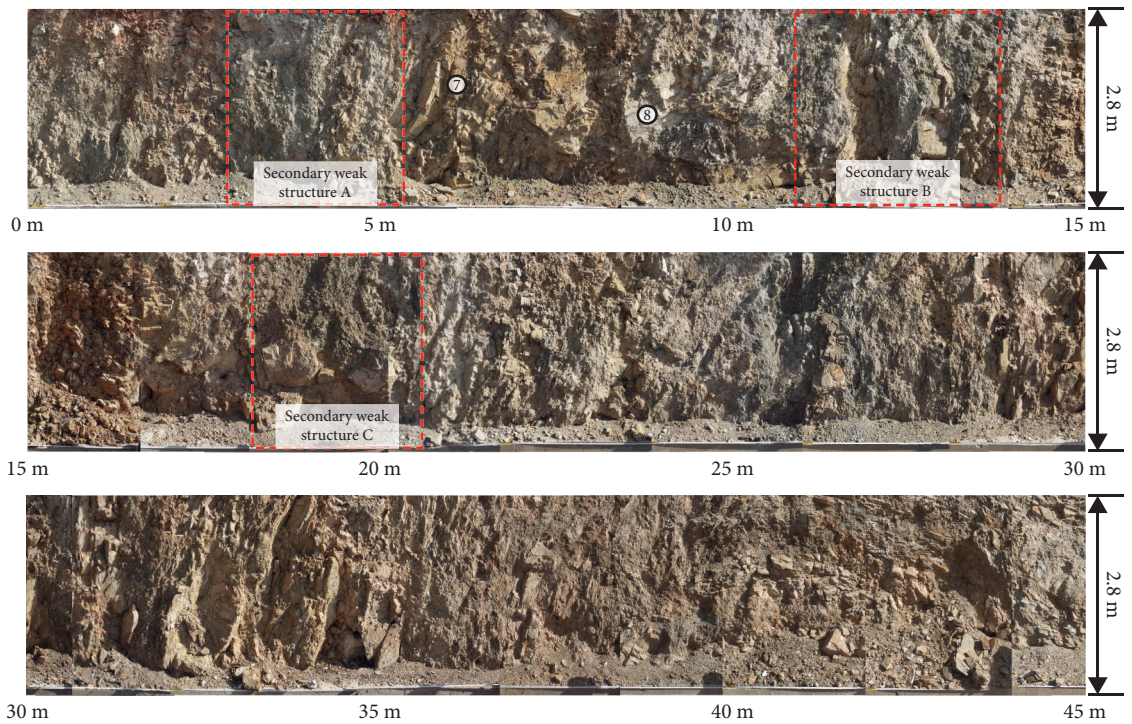

Figure 3: Outcrop profile of Jinshajiang main fault.

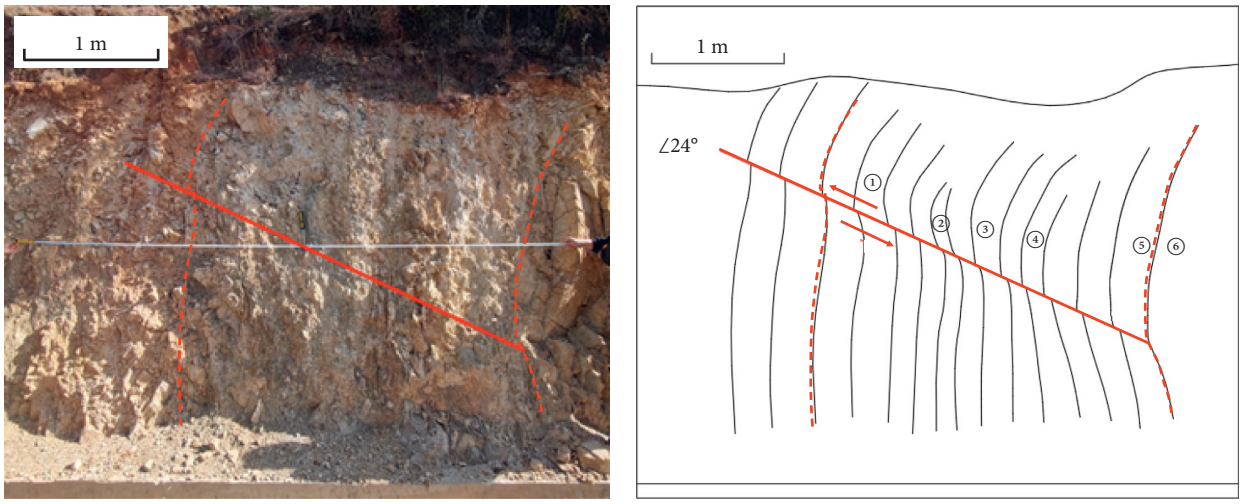

Figure 4: Outcrop of secondary weak structure A. (a). A photo of outcrop (b). A sketch of the outcrop.

main fault is significantly higher than that of the main structure to which the secondary weak structure belongs.

The whole rock minerals of 11 rock samples were analyzed by X-ray diffraction. The most abundant minerals are calcite, clay, and quartz, and the mineral contents are shown in Figure 10. The results show that, except for points 2, 3, and 9 of the secondary weak structures, the calcite content exceeds 80%, and the entire outcrop bedrock is limestone with similar mineral composition. The rock masses of the secondary weak structures have undergone geological process, and the mineral content and structure have changed, which is mainly manifested as an increase of clay mineral content. Points 2 and 9 are fault gouges, and the content of clay minerals reaches 37% and 65.1%, respectively.

3.4. Mechanical Properties of the Fracture Zone. Fault gouge is a typical secondary weak structure and also the mechanically weakest part of faulted rock mass [26]. Due to its large amount of clay minerals, the mechanical properties of the fault gouge are similar to those of clay. Geng et al. [27]

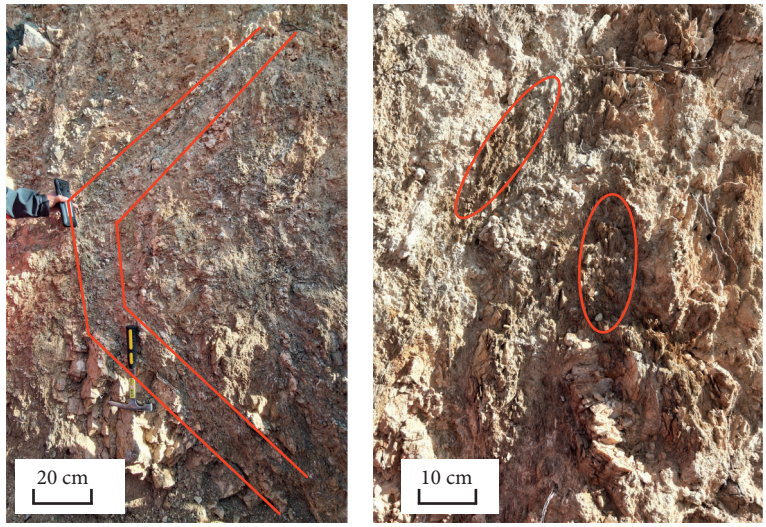

(a) (b)

Figure 5: Fault gouge and lens of secondary weak structure A. (a). Fault gouge (b). Lens.

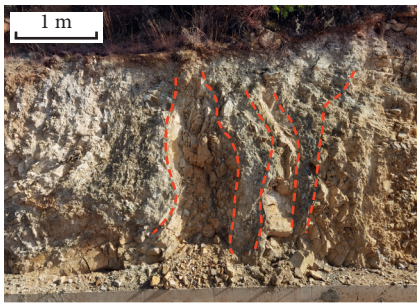

Figure 6: Outcrop of secondary weak structure B.

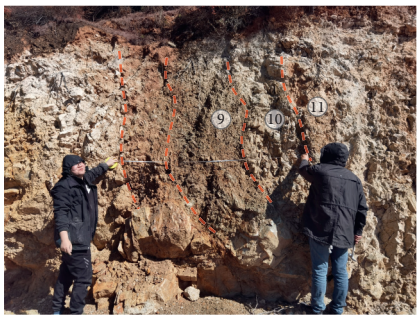

Figure 7: Outcrop of secondary weak structure C.

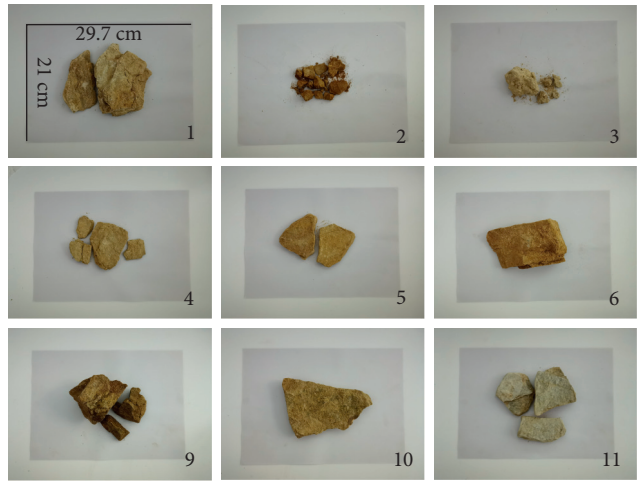

Figure 8: Rock samples of the secondary weak structures.

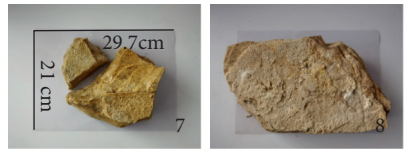

Figure 9: Rock samples of the fracture zone.

measured the mechanical parameters of fault gouge in five domestic fault zones. The maximum compressive strength is 5.16 MPa while the minimum is 1.78 MPa, with an average of 2.70 MPa. The maximum shear strength is 0.72 MPa while the minimum is 0.36 MPa, with an average of 0.53 MPa. The above data can provide a reference for the strength of fault gouge in this outcrop.

3.4.1. Point Load Test and Result Analysis. The degree of rock fragmentation is relatively high in the field, and it is difficult to prepare a large number of standard core samples. Therefore, point load tests are used to measure the macroscopic mechanical strength of the fracture zone. The point load samples are taken from points 7 and 8 in Figure 3 and are tested on the STDZ-3 digital display point load tester. After the point load strength is measured, it is converted into the point load strength index of the rock with an equivalent core diameter of 50 mm according to the standard for test methods for engineering rock mass [28], and then the macro uniaxial compressive strength of the rock is obtained by the following equation [29]:

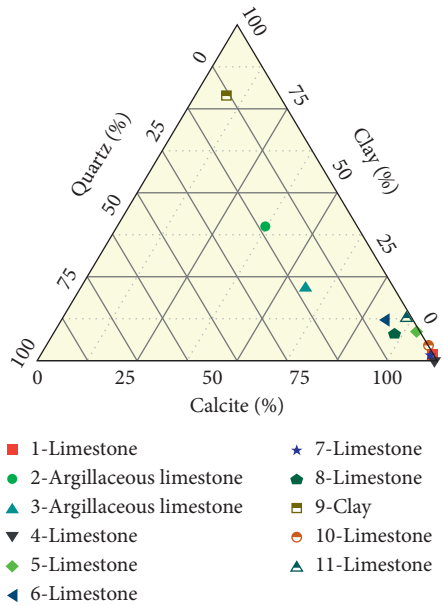

Figure 10: Mineral composition map of rock samples.

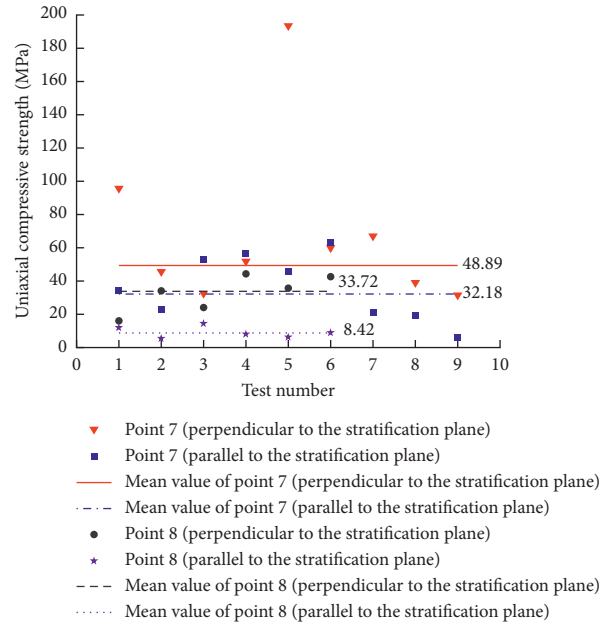

Figure 11: Uniaxial compressive strength of rock samples of the fracture zone.

$$R_c = 22.82 * \left(I_{s(50)}\right)^{0.75}. \quad (1)$$

R_c is the macroscopic uniaxial compressive strength of the rock; $I_{s(50)}$ is the point load strength index of the rock with a core diameter of 50 mm.

When the sample is subject to the wave velocity measurement test, it is found that the rock sample in the fracture zone has obvious anisotropy characteristics. The wave velocity of the parallel stratification plane and the perpendicular stratification plane at point 7 is 4.07 km/s and 2.30 km/s, respectively, whereas the wave velocity of the parallel stratification plane and the perpendicular stratification plane at point 8 is 3.94 km/s and 2.27 km/s, respectively. Therefore, the uniaxial compressive strength of the rock in the fracture zone is obtained by the average value after taking into account the effect of bedding distribution (0° and 90°, respectively, from the stratification plane) and filtering out the maximum and minimum values [28]. Figure 11 shows that the uniaxial compressive strength of the rock in the fracture zone has obvious anisotropy characteristics. Anisotropy index is an index reflecting the anisotropy of rock mass. The anisotropy index of rock point load strength is the ratio of vertical weak point load strength and parallel weak point load strength. For the rock at point 7, the uniaxial compressive strength in the vertical plane direction (48.89 MPa) is significantly greater than that in the parallel plane direction (32.18 MPa), and the anisotropy index is 1.52. For the rock at point 8, the uniaxial compressive strengths in the vertical and parallel plane directions are 33.72 MPa and 8.42 MPa, respectively, and the anisotropy index is 4.00. It shows that the anisotropy of the rock at point 8 in the fracture zone is obviously greater than that at point 7, which may be more likely to cause construction problems in practical projects.

3.4.2. Shear Test and Result Analysis. The rock is selected from the same area as the point load test, and the rock shear test is carried out. Considering the influence of the anisotropy of the bedding distribution, the shear mechanical properties of the rock in the fracture zone are analyzed.

The sample size of the shear test is a cube of $50 \times 50 \times 50$ mm. This shear test is carried out on a rock structural surface shear tester (RJST-616), in the displacement control mode of constant shear rate (3 mm/min). The loading stress path is to add the normal load to the target normal stress and then keep stable and apply the tangential load until the sample is broken. To obtain the approximate range of the shear strength of the rock in the outcrop fracture zone of the Jinshajiang main fault under the difficulty of sample processing, only the fixed normal stresses (5 MPa and 8 MPa) were used to conduct a shear test study parallel to and perpendicular to the plane in the shear test. Figure 12 shows the stress-displacement curve of the rock sample at point 7 under the normal stress of 5 MPa, perpendicular to the stratification plane and parallel to the stratification plane. When the rock is sheared in direction perpendicular to the stratification plane, the curve is concave at the beginning of loading and the cracks are compressed. Then the curve develops almost linearly. When the peak strength is approaching, the shear stress drops slightly. At this time, part of the layer has been sheared, and the specimen continues to be loaded to the peak strength (10.04 MPa). Then it enters the postpeak softening stage; the curve drops sharply and gradually reaches the residual shear strength, with the vertical layer of the rock being completely sheared. When the rock is sheared parallel to the stratification direction, the curve appears to be undulating and sawtooth at the beginning, since the set shear plane is not exactly parallel to the stratification plane, instead, with an angle of about 5°. With

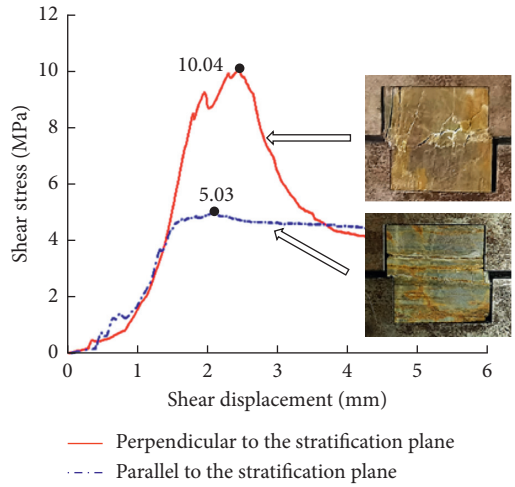

FIGURE 12: The curve of shear stress changing with shear displacement.

the loading of the tangential load, the peak shear stress reaches 5.03 MPa, and the shear stress drops little after the peak.

Represented by the shear strength perpendicularly and parallel to the stratification plane at points 7 and 8, the shear strength of the rock in the fracture zone is about 5.47~10.04 MPa when the normal stress is 5 MPa whereas it is about 10.08~31.72 MPa when the normal stress is 8 MPa.

4. Discussion on the Multilevel Structure of Jinshajiang Main Fault

The Batang section of Jinshajiang main fault is a typical multilevel structure, which consists of the primary structure and several secondary weak structures. The rock in the fracture zone is mainly massive limestone with calcite as the main component. The rock is layered and has a marked directivity. The uniaxial compressive strength of the rock in the fracture zone is about 8.42~48.89 MPa, and the shear strength under 5 MPa normal stress is about 5.47~10.04 MPa while the shear strength under 8 MPa normal stress is about 10.08~31.72 MPa. There are three secondary weak structures in the outcrop of the fracture zone, which are mainly composed of fault gouge and breccia. The particle size is relatively small, and the content of clay minerals is significantly higher than that of the rock mass in fracture zone. Represented by the strength of the conventional fault gouge, the difference between the strength value of the secondary fault gouge zone in the outcrop and the strength value of the fracture zone can reach an order of magnitude. In terms of geometrical morphology, mineral composition, and mechanical properties, the secondary weak structure in the fracture zone is significantly distinguished from the primary structure. The influence of the secondary weak structure cannot be ignored in geology and engineering.

In order to preliminarily discuss the influence of secondary soft structures on the displacement distribution, displacement concentration, and displacement gradient of rock strata on both sides of the section, a representative distributed structural fault and a multilevel structural fault model with secondary weak structures in the affected zone were constructed (Figure 13) for regular study. The construction of the model was based on the scale and rock mechanical parameters of Yuanmou-Lvzhijiang fault and other typical fault zones [30]. The overall size of the model is 100 m × 250 m × 100 m. The fault is set as a right-handed strike-slip fault with a 90° dip, and the relative creep rate of the two disks is 8 mm/a. The fault core of the fault model is simplified as a plane, and there is a secondary weak structure (at the coordinates of 75 m~80 m) in the left affected zone of the multilevel structure fault. The remaining structure and its size and parameters are the same as those of the distributed structure fault. The cross section of the tunnel is circular, the inner radius is 3.5 m, the primary and secondary lining are simplified to a lining structure with a thickness of 1.5 m, and the top of the tunnel is buried at a depth of 20 m. The elastic model is adopted in the hanging wall, the foot wall of rock mass, and the tunnel lining structure, and the Mohr-Coulomb model is adopted in the fault fracture zone, affected zone, and fault gouge. Some key structural mechanics parameters are shown in Table 1.

Fast Lagrange Analysis of Continua (FLAC3D) is used for numerical simulation. Figure 14 shows the tunnel displacement curve of distributed structure and multilevel structure under the working condition of 100 years of fault creeping 0.8 m relative total displacement of two discs. The displacement curve in the distributed fault shows an S-shaped distribution, and there is an inflection point at the junction of the fracture zone and the affected zone. The displacement gradient (curve slope) in the fracture zone is significantly greater than that in the affected zone. The simulation results are basically with the displacement model of strike-slip fault simulated by Xue et al. [30]. In the multilevel structural fault, the overall displacement pattern still presents an "S"-shaped distribution, but the axial offset distance of the tunnel is no longer symmetrical according to the center of the main sliding surface. The relative displacement within the width of 50~125 m is greater than that within the width of 125~200 m. The displacement gradient at the inflection point (the interface between the fracture zone and the affected zone) is significantly reduced, the relative dislocation amount at the secondary weak structure is significantly increased, and the displacement gradient at 80–100 m in the affected zone is significantly increased.

The above numerical simulation is only for a multilevel structural fault with a secondary weak structure in the affected zone. It aims to show the overall displacement pattern of multilevel structural fault and explain the influence of the secondary weak structure on the overall displacement distribution. In the multilevel structure, the difference in the composition of the clay minerals between the secondary weak structure and the primary structure and the difference in the crack density make the mechanical properties of the two quite different. At the same time, the width, number, and distribution of the secondary weak structure will affect the distribution of fault displacement and tunnel stress, which need to be analyzed

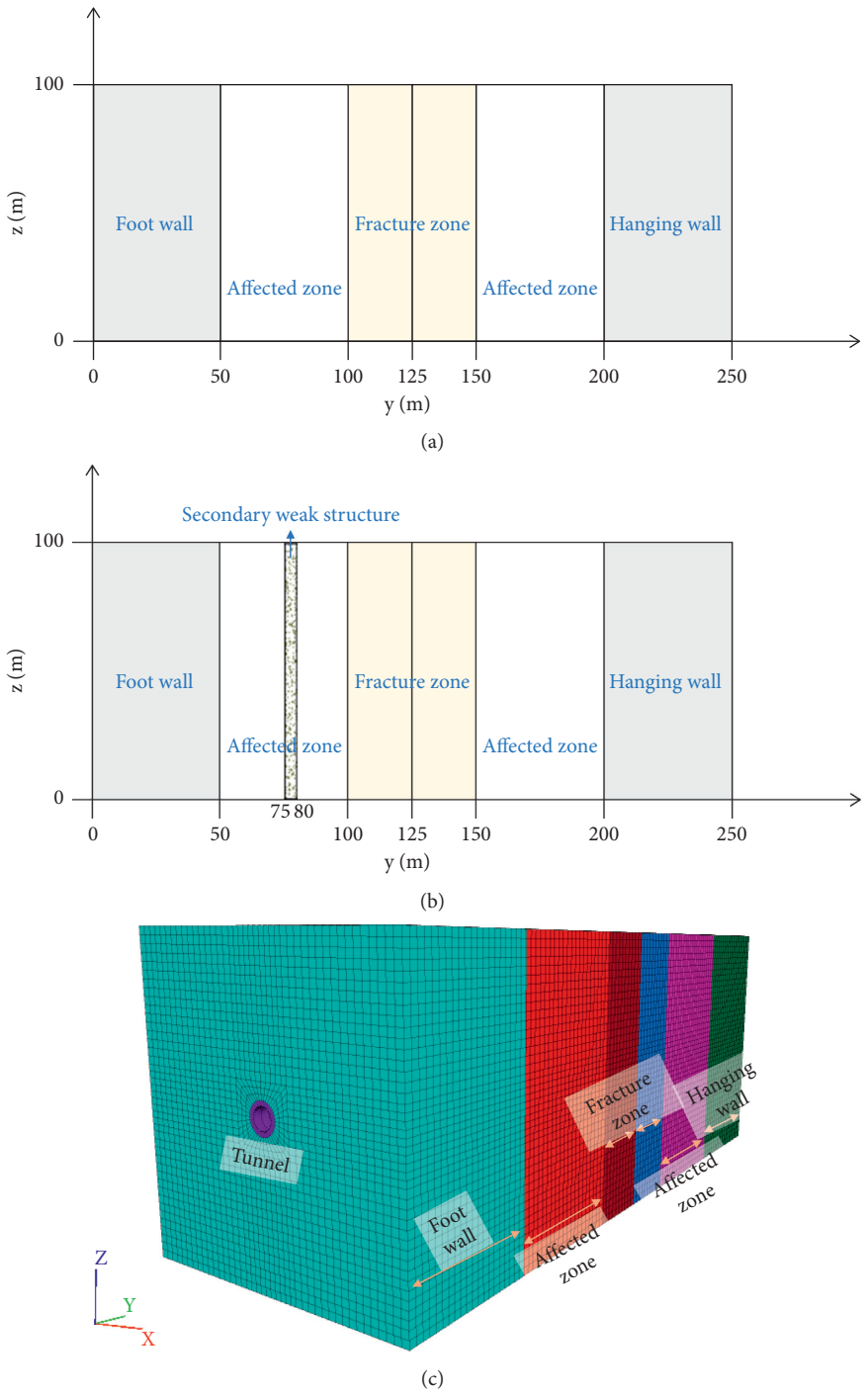

Figure 13: Diagram of numerical simulation model. (a) Schematic diagram of the distributed structure fault. (b) Schematic diagram of multilevel structure fault. (c) Tunnel-distributed fault model.

Table 1: The mechanical parameters of each structure in the fault model [30].

Structure	Bulk modulus (Pa)	Shear modulus (Pa)	Cohesion (Pa)	Internal friction angle (o)
Hanging wall and foot wall	4.448e9	2.417e9	—	—
Affected zone	3.090e9	1.551e9	1.26e6	32
Fracture zone	6.370e9	0.228e9	0.41e6	26.4
Secondary weakness structure	0.556e9	0.185e9	0.3e6	20
Lining	1.944e9	14.583e9	—	—

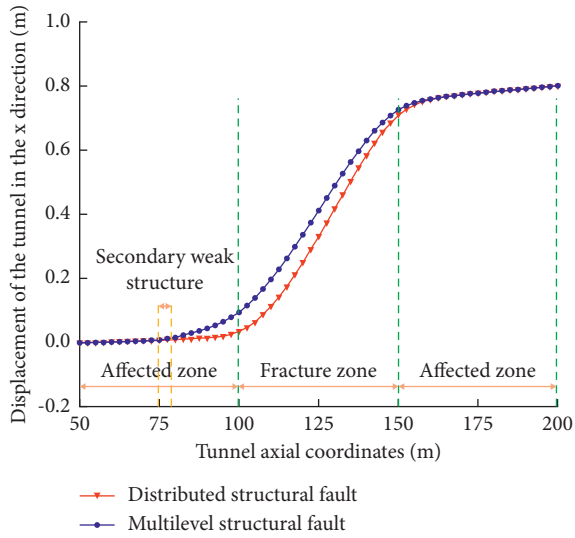

Figure 14: Displacement curves of tunnel across distributed structure and multilevel structure.

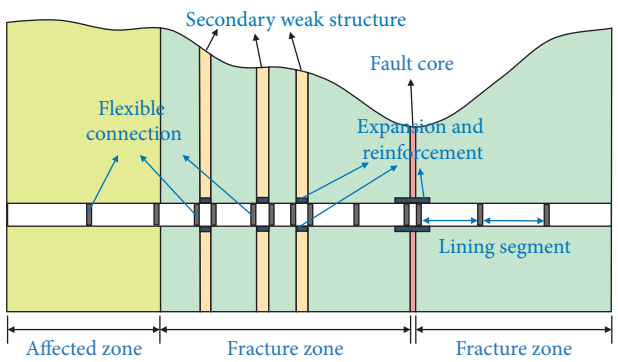

Figure 15: Engineering measures for tunnel crossing multilevel structural fault.

in detail later. From the perspective of engineering response, for tunnel projects that traverse distributed structures or centralized structural faults, the commonly adopted measures at present include the expansion and reinforcement of the tunnel passing through the center of the fault and equal-distance sectioning of the tunnel lining [31, 32]. However, for tunnel projects that cross the Jinshajiang main fault or other multilevel structural faults, it is also recommended to focus on strengthening the secondary weak structures (Figure 15). Reinforcement can be done by pouring concrete or using new materials [33, 34]. If the tunnel adopts the method of lining subsections, the tunnel lining nodes can be designed according to the distribution of the main structure and the number and position of the secondary weak structure, which should follow the principle that the connecting segment should be set where the distance between the lining segments is small and that the displacement gradient changes where the displacement is large. For example, in Figure 15, flexible connecting sections are set at the junction of the fracture zone and the affected zone, the secondary weak structure, and the main structure, and the nonequidistant lining section method is adopted to achieve the purpose of safe and economical construction.

5. Conclusions

(1) The fault multilevel structure is proposed from the perspective of engineering and mechanics, which refers to the primary structure and the secondary weak structure. The secondary weak structure is the area with weak mechanical property where the fault is subordinate to the primary structure, such as cleavage narrow band, joint narrow band, fault gouge band, and small fold. Its main components are fault gouge, granular rock, and breccia. The rock mass is loose and broken, and the strength is low.

(2) The Batang section of Jinshajiang main fault is a typical fault multilevel structure. There are three secondary weak structures in the investigation area of the fracture zone. One is a small fault with a narrow zone of fault gouge, one is a limestone zone and fault gouge zone with dense joints, and the other is a fault gouge zone. The secondary weak structure can be distinguished by rock geometrical morphology, mineral composition, and mechanical properties.

(3) Different periods of the tectonic movement led to the formation of fault multilevel structure. The overall displacement pattern of multilevel structural fault presents S-shaped distribution. The secondary weak structure will affect the displacement distribution and displacement gradient, and the fault concentration position will shift towards the secondary weak structure. During the creeping process of the fault, the secondary weak structure also has the possibility of slipping. In the tunnel project crossing active faults, it is recommended to strengthen the secondary weak structure; if the tunnel adopts lining sectioning measures, the section distance and node position of the secondary weak structure can be adjusted with the displacement mode.

(4) The multilevel structure of the fault, together with centralized structure, distributed structure, and stepped structure of the fault, can be used as a structure classification method of fault structure. In the follow-up research on fault prevention of tunnels crossing active faults, it is necessary to fully consider the structural characteristics of the faults, refine fault models, and study tunnel failure mechanism with more accurate displacement mode for precise prevention and control.

Data Availability

No data were used to support this study.

Conflicts of Interest

The authors declare that they have no conflicts of interest.

References

[1] M. C. He, *National Natural Science Foundation of Sichuan-Tibet Railway Major Special Project–Sichuan-Tibet Railway Deep Buried Ultra-long Tunnel Project Disaster Mechanism and Prevention and Control Methods*China University of Mining and Technology, Beijing), 2020.

[2] D. Closson, N. Abou Karaki, N. Milisavljević, F. Hallot, and M. Acheroy, "Salt tectonics of the lisan diapir revealed by synthetic aperture radar images," in *Tectonics*, D. Closson, Ed., pp. 303–328 Intech, Malden, MA, USA, 2011.

[3] Z. K. Shipton, J. P. Evans, and L. B. Thompson, "The geometry and thickness of deformation-band fault core and its influence on sealing characteristics of deformation-band fault zones," *AAPG Memoir*, vol. 85, 2005.

[4] H. Fossen and J. Hesthammer, "Possible absence of small faults in the Gullfaks Field, northern North Sea: implications for downscaling of faults in some porous sandstones," *Journal of Structural Geology*, vol. 22, no. 7, pp. 851–863, 2000.

[5] I. R. Brown, T. L. Brekke, and G. E. Korbin, *Behavior Of the Bay Area Rapid Transit Tunnels Through the Hayward Fault (No. UMTA-CA-06-0120-81-1Final Rpt*, California, FL, USA, 1981.

[6] L. X. Xiong, *Numerical Simulation of Seismic Resistance of Tunnel in Active Fault Area*, Chengdu University of Technology. College of Environmental and Civil Engineering, Chengdu, 2006.

[7] D. R. Faulkner, T. M. Mitchell, E. H. Rutter, and J. Cembrano, "On the structure and mechanical properties of large strike-slip faults," *Geological Society, London, Special Publications*, vol. 299, no. 1, pp. 139–150, 2008.

[8] H. E. Demirci, S. Bhattacharya, D. Karamitros, and N. Alexander, "Experimental and numerical modelling of buried pipelines crossing reverse faults," *Soil Dynamics and Earthquake Engineering*, vol. 114, pp. 198–214, 2018.

[9] M. Sabagh and A. Ghalandarzadeh, "Numerical modelings of continuous shallow tunnels subject to reverse faulting and its verification through a centrifuge," *Computers and Geotechnics*, vol. 128, Article ID 103813, 2020.

[10] M. S. Abdollahi, M. Najafi, A. Y. Bafghi, and M. F. Marji, "A 3D numerical model to determine suitable reinforcement strategies for passing TBM through a fault zone, a case study: safaroud water transmission tunnel, Iran," *Tunnelling and Underground Space Technology*, vol. 88, pp. 186–199, 2019.

[11] X. Y. Liu, C. Q. Zhang, T. Y. Shi et al., "Experimental study of axial displacements mode of deep buried tunnel across active faults," *Rock and Soil Mechanics*, vol. 42, no. 05, pp. 1304–1312, 2021.

[12] H. Fossen, *Structural Geology*, United States of America by Cambridge University Press, New York, NY, USA, 2010.

[13] D. R. Faulkner, C. A. L. Jackson, R. J. Lunn et al., "A review of recent developments concerning the structure, mechanics and fluid flow properties of fault zones," *Journal of Structural Geology*, vol. 32, no. 11, pp. 1557–1575, 2010.

[14] J. W. Xia and M. Zhu, "Study on tectonic characteristics and activity in the middle part of Jinshajiang main fault zone," *Yangtze River*, vol. 51, no. 05, 2020.

[15] Y. Q. Chang, L. C. Chen, and Q. Zhang, "Study on tectonic landform and fault activity characteristics of Jinshajiang fault zone," *Journal of International Seismology*, no. 08, pp. 142-143, 2019.

[16] B. Yuan, Z. Li, Z. Zhao, H. Ni, Z. Su, and Z. Li, "Experimental study of displacement field of layered soils surrounding laterally loaded pile based on transparent soil," *Journal of Soils and Sediments*, vol. 21, no. 9, pp. 3072–3083, 2021.

[17] B. Yuan, M. Sun, L. Xiong, Q. Luo, S. P. Pradhan, and H. Li, "Investigation of 3D deformation of transparent soil around a laterally loaded pile based on a hydraulic gradient model test," *Journal of Building Engineering*, vol. 28, Article ID 101024, 2020.

[18] B. Yuan, Z. Li, Z. Su, Q. Luo, M. Chen, and Z. Zhao, "Sensitivity of multistage fill slope based on finite element model," *Advances in Civil Engineering*, vol. 2021, Article ID 6622936, 13 pages, 2021.

[19] P. Guo, X. Gong, Y. Wang, H. Lin, and Y. Zhao, "Minimum cover depth estimation for underwater shield tunnels," *Tunnelling and Underground Space Technology*, vol. 115, Article ID 104027, 2021.

[20] P. Guo, X. Gong, and Y. Wang, "Displacement and force analyses of braced structure of deep excavation considering unsymmetrical surcharge effect," *Computers and Geotechnics*, vol. 113, Article ID 103102, 2019.

[21] M. Zaheri, M. Ranjbarnia, D. Dias, and P. Oreste, "Performance of segmental and shotcrete linings in shallow tunnels crossing a transverse strike-slip faulting," *Transportation Geotechnics*, vol. 23, Article ID 100333, 2020.

[22] C. Chengfa, C. Nansheng, M. P. Coward et al., "Preliminary conclusions of the royal society and academia sinica 1985 geotraverse of tibet," *Nature*, vol. 323, no. 6088, pp. 501–507, 1986.

[23] Z. F. Chang, H. Chang, and Y. Zang, "Recent active features of Weixi-Qiaohou fault and its relationship with the Honghe fault," *Journal of Geomechanics*, vol. 22, no. 3, pp. 517–530, 2016.

[24] X. X. Xu, L. Y. Ji, F. Y. Jiang, and W. T. Zhang, "Study on current activity features of Jinshajiang Fault Zone based on GPS and small earthquakes," *Journal of Geodesy and Geodynamics*, pp. 1062–1067, 2020.

[25] F. G. Huang, "The relationship between the thickness and grain size of fault gouge and fault dislocation," *Earthquake Research in Sichuan*, no. 01, pp. 50–56, 1998.

[26] M. M. Wang, J. W. Liu, D. Y. Wang, Y. Zhu, and Z. L. Nie, "Study on bearing capacity and deformation characteristics of fault rock mass," *Science Technology and Engineering*, vol. 20, no. 23, pp. 9556–9550, 2020.

[27] N. G. Geng, X. X. Yao, and Y. Chen, "Preliminary study on mechanical properties of five faults gouge in China," *Earthquake Research in China*, no. 04, pp. 62–67, 1985.

[28] China Electricity Council, *Standard for Test Methods for Engineering Rock Mass*, GB/T 50266-2013, China Planning Press, Beijing, China, 2013.

[29] Ministry of Water Resources of the People's Republic of China, *Standard for Test Methods for Engineering Rock Mass*, GB 50218-94, China Planning Press, Beijing, China, 1995.

[30] S. Q. Xue, C. Q. Zhang, C. Z. Xiao et al., "Study on creep displacement model of active fault in water conveyance tunnel," *Yangtze River*, vol. 50, no. 11, pp. 149–155, 2019.

[31] R. Caulfield, D. S. Kieffer, D. F. Tsztoo, and B. Cain, *Seismic Design Measures for the Retrofit of the claremont Tunnel*, RETC Proceedings California, The Rapid Excavation and Tunneling Conference (RETC), California, FL, USA, 2005.

[32] A. R. Shahidi and M. Vafaeian, "Analysis of longitudinal profile of the tunnels in the active faulted zone and designing the flexible lining (for Koohrang-III tunnel)," *Tunnelling and Underground Space Technology*, vol. 20, no. 3, pp. 213–221, 2005.

[33] B. Yuan, Z. Li, Y. Chen et al., "Mechanical and microstructural properties of recycling granite residual soil reinforced with glass fiber and liquid-modified polyvinyl alcohol polymer," *Chemosphere*, vol. 286, Article ID 131652, 2022.

[34] M. C. He, C. Li, W. L. Gong, J. Wang, and Z. Tao, "Support principles of NPR bolts/cables and control techniques of large deformation," *Chinese Journal of Rock Mechanics and Engineering*, vol. 35, no. 8, pp. 1513–1529, 2016.